Tethered Pyrazolyl Phosphinate: Pyrazolyl-*N*- and Phosphoryl-*O*-Metal Coordination in $Ph_2P(O)\{OCH_2CH_2(3,5\text{-}Me_2Pz)\}$

Savariraj Kingsley,[†] Vadapalli Chandrasekhar,*[,†] Christopher D. Incarvito,[‡] Matthew K. Lam,[‡] and Arnold L. Rheingold[‡]

Department of Chemistry, Indian Institute of Technology, Kanpur-208016, India, and Department of Chemistry and Biochemistry, University of Delaware, Newark, Delaware 19716

Received April 30, 2001

Phosphorus pyrazolides, $P(O)(3,5\text{-}Me_2Pz)_3$ or $RP(E)(3,5\text{-}Me_2Pz)_2$ [E = S or O, R = Me or Ph], are hydrolytically sensitive particularly upon interaction with transition metal ions. In this paper, we report a new tethered pyrazolyl phosphinate, $Ph_2P(O)\{OCH_2CH_2(3,5\text{-}Me_2Pz)\}$ DPEP (**1**), where the pyrazolyl group is separated from the phosphorus by means of an ethyleneoxy spacer. **1** has two potential coordination sites in the form of a phosphoryl oxygen atom and a pyrazolyl nitrogen atom. **1** forms hydrolytically stable complexes, $(DPEP{\cdot}CoCl_2)_n$ (**2**), $(DPEP)_2{\cdot}CuCl_2$ (**3**), $(DPEP{\cdot}ZnCl_2)_n$ (**4**), and $(DPEP)_2{\cdot}PdCl_2$ (**5**). The cobalt(II) and the zinc(II) complexes **2** and **4** show a zigzag polymeric structure in the solid state with a tetrahedral coordination geometry around the metal ion; the ligand DPEP coordinates through its phosphoryl oxygen and the pyrazolyl nitrogen to two neighboring metal ions and functions as a bridging ligand to form the polymeric structure. In contrast to **2** and **4**, the copper(II) and the palladium(II) complexes **3** and **5** show a square-planar geometry around the metal ion. Exclusive coordination through the pyrazolyl nitrogens of the ligand **1** is observed. An extensive supramolecular sheetlike two-dimensional polymeric network is observed in the solid-state structures of **3** and **5** as a result of two weak interactions: (a) an intermolecular C−H- - -O interaction involving the phosphoryl oxygen and an aromatic C−H and (b) a $\pi-\pi$ face-to-face stacking interaction between the phenyl groups of two adjacent molecules.

Introduction

In contrast to the well-studied family of polypyrazolyl borate ligands,[1] the corresponding ligands based on phosphorus have not received as much attention.[2] One of the difficulties in the use of the latter family, where the pyrazolyl group is attached to the phosphorus through the nitrogen atom, is the susceptibility of the resultant P−N bond toward hydrolysis particularly upon interaction with transition metal ions.[2a] In this context, recently we have reported an unusual desulfurization of bis(3,5-dimethylpyrazolyl)methylphosphine sulfide, $MeP(S)(3,5\text{-}Me_2Pz)_2$.[3] This ligand, upon interaction with $CuCl_2$, affords a tetranuclear copper(II) cluster, where the four copper atoms are held together by an in situ formed methylphosphonate, $MePO_3^{2-}$. This reaction is triggered by a metal-assisted P−N bond hydrolysis involving the phosphorus−pyrazole linkage.[3] Partial hydrolysis reactions involving these ligand systems are also known. Thus, the reaction of tris(3,5-dimethylpyrazolyl)phosphine oxide, $P(O)(3,5\text{-}Me_2Pz)_3$, with $Cu(ClO_4)_2{\cdot}2H_2O$ leads to the product $[\{P(O)_2(3,5\text{-}Me_2Pz)_2\}_2{\cdot}Cu]$, where one of the pyrazolyl groups is hydrolyzed, and the in situ generated anionic phosphinate ligand acts in a tridentate manner using a N_2O coordination mode.[4] Such a partial hydrolysis also occurs in the reaction with a molybdenum carbonyl derivative.[2a] Similarly, the reaction of 3-(2-pyridyl)pyrazole with $POBr_3$ does not afford the expected tris(pyrazolyl)phosphine oxide but affords the partially hydrolyzed product bis[3-(2-pyridyl)pyrazol-1-yl]phosphinate.[2e] Examples of partial P−N bond hydrolysis are also documented in cyclic phosphazenes involving pyrazolyl derivatives such as $N_3P_3(3,5\text{-}Me_2Pz)_6$[5] or aminocyclophosphazenes such as $N_3P_3(HNCH_2CH_2NH)(NMe_2)_4$.[6] One of the ways of preparing robust ligands of this family where the problem of P−N bond hydrolysis is avoided is to incorporate a spacer between the pyrazolyl substituent and the phosphorus. To test this idea, we have synthesized *P*,*P*-diphenyl-2-{3,5-dimethylpyrazol-1-yl}-ethylphosphinate, $Ph_2P(O)\{OCH_2CH_2(3,5\text{-}Me_2Pz)\}$, hereafter called DPEP (**1**), and studied its coordination behavior toward

[†] Indian Institute of Technology.
[‡] University of Delaware.

(1) Review and representative examples: (a) Trofimenko, S. *Chem. Rev.* **1993**, *93*, 943. (b) Seino, H.; Arai, Y.; Iwata, N.; Nagao, S.; Mizobe, Y.; Hidai, M. *Inorg. Chem.* **2001**, *7*, 1677. (c) Lopes, I.; Hillier, A. C.; Liu, S. Y.; Domingos, A.; Ascenso, J.; Galvão, A.; Sella, A.; Marques, N. *Inorg. Chem.* **2001**, *6*, 1116. (d) Hu, Z.; Gorun, S. M. *Inorg. Chem.* **2001**, *4*, 667. (e) Rasika Dias, H. V.; Lu, H. L. *Inorg. Chem.* **2000**, *10*, 2246. (f) Kimblin, C.; Bridgewater, B. M.; Churchill, D. G.; Hascall, T.; Parkin, G. *Inorg. Chem.* **2000**, *19*, 4240. (g) Long, D. P.; Chandrasekaran, A.; Day, R. O.; Bianconi, P. A.; Rheingold, A. L. *Inorg. Chem.* **2000**, *20*, 4476. (h) Komatsuzaki, H.; Nagasu, Y.; Suzuki, K.; Shibasaki, T.; Satoh, M.; Ebina, F.; Hikichi, S.; Akita, M.; Moro-oka, Y. *J. Chem. Soc., Dalton Trans.* ***1998***, 511. (i) Akita, M.; Ohta, K.; Takahashi, Y.; Hikichi, S.; Moro-oka, Y. *Organometallics* **1997**, *16*, 4121. (j) Kitajima, N.; Fujisawa, K.; Moro-oka, Y. *J. Am. Chem. Soc.* **1990**, *8*, 3210.

(2) (a) Joshi, V. S.; Kale, V. K.; Sathe, K. M.; Sarkar, A.; Tavale, S. S.; Suresh, C. G. *Organometallics* **1991**, *10*, 2898. (b) Tokar, C. J.; Kettler, P. B.; Tolman, W. B. *Organometallics* **1992**, *8*, 2737. (c) Chowdhury, S. K.; Joshi, V. S.; Samuel, A. G.; Puranik, V. G.; Tavale, S. S.; Sarkar, A. *Organometallics* **1994**, *13*, 4092. (d) LeCloux, D. D.; Tokar, C. J.; Osawa, M.; Houser, R. P.; Keyes, M. C.; Tolman, W. B. *Organometallics* **1994**, *13*, 2855. (e) Psillakis, E.; Jeffery, J. C.; McCleverty, J. A.; Ward, M. D. *J. Chem. Soc., Dalton Trans.* **1997**, 1645.

(3) Chandrasekhar, V.; Kingsley, S.; Vij, A.; Lam, K. C.; Rheingold, A. L. *Inorg. Chem.* **2000**, *39*, 3238.

(4) Chandrasekhar, V.; Nagendran, S.; Kingsley, S.; Krishnan, V.; Boomishankar, R. *Proc.-Indian Acad. Sci., Chem. Sci.* **2000**, *112*, 171.

(5) Thomas, K. R. J.; Chandrasekhar, V.; Scott, S. R.; Hallford, R.; Cordes, A. W. *J. Chem. Soc., Dalton Trans.* **1993**, 2589.

(6) Chandrasekaran, A.; Krishnamurthy, S. S.; Nethaji, M. *Inorg. Chem.* **1994**, *33*, 3085.

10.1021/ic010454c CCC: $20.00
Published on Web 10/05/2001

Co(II), Cu(II), Zn(II), and Pd(II) chlorides. We describe here the details of the above investigations involving the synthesis, X-ray structural characterization, and spectroscopy of the tethered pyrazolyl phosphinate **1** and its transition metal complexes **2**−**5**.

Experimental Section

Reagents and General Procedures. The solvents were purified and were dried according to standard procedures.[7] Anhydrous cobalt(II) chloride, copper(II) chloride, zinc(II) chloride, palladium(II) chloride bisbenzonitrile, diphenylphosphinic chloride, and 2-chloroethanol were acquired from Fluka, Switzerland, and were used as such. Triethylamine (Qualigens, India) was dried over KOH and was freshly distilled before use. 3,5-Dimethylpyrazole[7] and 1-(hydroxyethyl)-3,5-dimethylpyrazole[8] were prepared according to literature procedures.

Instrumentation. Infrared spectra were recorded as KBr pellets using a Bruker Vector 22 FTIR spectrophotometer. ^{1}H and ^{31}P NMR spectra were recorded on a JEOL spectrometer operating at 400 and 135 MHz, respectively. EPR spectra were recorded on a Varian spectrometer at X-band frequency, and the magnetic field was calibrated with DPPH. Optical absorption spectra were obtained by using 1-cm quartz cells in a Shimadzu UV-160 spectrophotometer. Mass spectra were recorded on a JEOL Sx 102/DA 6000 mass spectrometer using xenon (6 kV, 10 mA) as the FAB gas. Electron spray mass spectra were recorded on a MICROMASS QUATTRO II triple quadrupole mass spectrometer in dichloromethane solution. C, H, and N analysis were carried out at the Central Drug Research Institute's (Lucknow, India) regional instrumentation facility. Magnetic susceptibility data were obtained for polycrystalline samples of **2** and **3** using a locally built magnetometer. The setup consists of an electromagnet with constant gradient pole caps (Polytronic Corp., Mumbai, India) and a Sartorius M25-D/S balance (Germany). $Hg[Co(NCS)_4]$ was used as the calibrant. All of the preparative procedures described in the following were carried out under an inert gas atmosphere of dry N_2.

Synthesis of DPEP (1). Diphenyl phosphinic chloride (7.57 g, 31.99 mmol) dissolved in 25 mL of THF was added dropwise to an ice cold solution of 2-ethoxy-3,5-dimethylpyrazole (4.48 g, 31.95 mmol) and triethylamine (3.24 g, 32.01 mmol) in 150 mL of dry THF. The reaction mixture was allowed to attain room temperature and then was heated under reflux for 24 h. It was again allowed to attain room temperature, was filtered, and the solvent was removed from the filtrate in vacuo affording a white solid. This was recrystallized from a mixture of *n*-hexane and benzene (10:1) at 25 °C to afford white needles of DPEP (9.20 g, 85%): mp 90 °C. IR (KBr): 3074 (s), 2969 (s), 2947 (s), 2919 (s), 1588 (s), 1553 (s), 1458 (s), 1438 (s), 1381 (s), 1311 (s), 1223 (vs), 1130 (vs), 1082 (vs), 1041 (vs), 934 (vs), 784 (s), 731 (vs), 695 (s), 562 (s) cm^{-1}. IR (CH_2Cl_2): 3049 (m), 2949 (m), 1590 (w), 1553 (m), 1438 (m), 1385 (w), 1266 (m), 1226 (s), 1130 (s), 1072 (s), 1040 (s), 937 (m), 786 (w), 732 (s), 696 (s), 561 (s), 535 (s) cm^{-1}. ^{1}H NMR ($CDCl_3$, ppm): δ 7.68−7.35 (m, 10H, *Phenyl*), 5.84 (s, 1H, *4H*−*Pyrazole*), 4.33 (d, 4H, *OCH*$_2$*CH*$_2$*N*), 2.24 (s, 3H, *CH*$_3$), 2.21 (s, 3H, *CH*$_3$). ^{31}P NMR ($CDCl_3$, ppm): δ 32.9 (s). Mass spectrum (FAB): 341.4 (M^+). Anal. Calcd for $C_{19}H_{21}N_2O_2P$ (340.35): C, 67.05; H, 6.22; N, 8.23. Found: C, 66.82; H, 6.35; N, 8.03.

Synthesis of (DPEP·CoCl$_2$)$_n$ (2). Anhydrous $CoCl_2$ (0.13 g, 1.0 mmol) was added to a solution of **1** (0.34 g, 0.99 mmol) in dichloromethane (50 mL). The reaction mixture was stirred at room temperature for 10 h. It was filtered, and the solvent was removed from the filtrate to afford a blue crystalline powder (0.38 g, 81%): mp 168 °C. IR (KBr): 3441 (w), 3050 (m), 2966 (m), 1589 (m), 1551 (s), 1468 (s), 1437 (s), 1396 (s), 1379 (m), 1310 (m), 1262 (m), 1224 (s), 1191 (vs), 1130 (s), 1111 (s), 1077 (s), 1018 (s), 954 (s), 795 (s), 756 (s), 730 (m), 695 (s), 568 (s), 536 (s) cm^{-1}. IR (CH_2Cl_2): 3055 (m), 2962 (m), 2926 (m), 1591 (w), 1553 (m), 1438 (s), 1374 (w), 1309 (w), 1262 (m), 1181 (s), 1112 (s), 1074 (s), 1038 (vs), 939 (s), 798 (m), 732 (s), 696 (s), 562 (s), 534 (s), 505 (s) cm^{-1}. UV−vis {CH_2Cl_2, [λ_{max}/nm (ϵ_{max}/M^{-1} cm^{-1})]}: 665 (334), 640 (sh, 300), 590 (191), 266 (1901), 246 (2263). Mass (ESMS, CH_2Cl_2): 905.1[(DPEP)$_2$·COCl$_2$·CoCl]$^+$. Anal. Calcd for $C_{19}H_{21}Cl_2CoN_2O_2P$ (470.18): C, 48.53; H, 4.50; N, 5.90. Found: C, 48.49; H, 4.55; N, 6.08. Solid-state room-temperature magnetic susceptibility measurement gives μ_{eff} per Co as 4.20 μ_B.

Synthesis of (DPEP)$_2$·CuCl$_2$ (3). Anhydrous $CuCl_2$ (0.13 g, 0.96 mmol) was added to a solution of **1** (0.68 g, 1.99 mmol) in dichloromethane (60 mL). The resulting green solution was stirred at room temperature for 10 h. This was filtered, and the solvent was removed from the filtrate to afford a green solid (0.75 g, 92.5%): mp 124 °C. IR (KBr): 3055 (m), 2960 (m), 1590 (m), 1552 (s), 1465 (s), 1438 (s), 1384 (s), 1312 (s), 1261 (s), 1226 (vs), 1129 (vs), 1110 (vs), 1038 (vs), 939 (s), 801 (s), 752 (s), 728 (s), 695 (s), 562 (s), 535 (s) cm^{-1}. IR (CH_2Cl_2): 3051 (m), 2961 (m), 2854 (m), 1592 (w), 1554 (m), 1438 (m), 1395 (m), 1310 (sh, w), 1265 (s), 1223 (s), 1130 (s), 1112 (s), 1038 (s), 939 (m), 864 (w), 797 (m), 736 (s), 698 (s), 560 (m), 532 (m), 499 (m) cm^{-1}. UV−vis {CH_2Cl_2, [λ_{max}/nm (ϵ_{max}/M^{-1} cm^{-1})]}: 883 (106), 377 (1264), 273 (5000), 239 (4754). EPR (CH_2Cl_2/toluene, 1:1, 300 K): broad isotropic signal with half line width of 195G and g_{iso} of 2.135. EPR (CH_2Cl_2/toluene, 1:1, 77 K): $g_{||}$, 2.37; $A_{||}$, 93.23 × 10^{-4} cm^{-1}; $g_{\perp}$, 2.10. Anal. Calcd for $C_{38}H_{42}Cl_2CuN_4O_4P_2$ (815.15): C, 55.99; H, 5.19; N, 6.87. Found: C, 56.02; H, 5.26; N, 6.96. Solid-state room-temperature magnetic susceptibility measurement gives a μ_{eff} per Cu as 1.92 μ_B. Solution magnetic susceptibility measurement (Evans NMR method, chloroform as solvent) gave a value of 1.90 μ_B.

Synthesis of (DPEP·ZnCl$_2$)$_n$ (4). Anhydrous $ZnCl_2$ (0.14 g, 1.02 mmol) was added to a solution of **1** (0.34 g, 0.99 mmol) in dichloromethane (50 mL). The resulting colorless solution was stirred at room temperature for 10 h. This was filtered, and from the filtrate the solvent was removed in vacuo to afford a white crystalline powder (0.40 g, 84%): mp 240 °C. IR (KBr): 3056 (m), 2959 (m), 1590 (m), 1554 (s), 1466 (s), 1438 (s), 1389 (s), 1375 (sh, m), 1310 (w), 1273 (w), 1179 (vs), 1133 (s), 1112 (s), 1073 (s), 1040 (vs), 995 (sh, m), 945 (s), 796 (m), 752 (m), 733 (vs), 694 (s), 563 (s), 536 (s) cm^{-1}. IR (CH_2Cl_2): 3054 (m), 2925 (m), 1590 (m), 1554 (m), 1467 (sh, m), 1438 (s), 1374 (m), 1310 (w), 1268 (w), 1180 (s), 1133 (s), 1112 (s), 1073 (sh, m), 1040 (s), 945 (m), 796 (sh, m), 733 (s), 695 (s), 562 (s), 535 (s) cm^{-1}. ^{1}H NMR ($CDCl_3$, ppm): δ 7.82−7.49 (m, 10H, *Phenyl*), 5.94 (s, 1H, *4H*−*Pyrazole*), 4.28 (d, 4H, *OCH*$_2$*CH*$_2$*N*), 2.41 (s, 3H, *CH*$_3$), 2.26 (s, 3H, *CH*$_3$). ^{31}P NMR ($CDCl_3$, ppm): δ 38.8 (s). Mass (ESMS, CH_2Cl_2): 917[(DPEP)$_2$·ZnCl$_2$·ZnCl]$^+$. Anal. Calcd for $C_{19}H_{21}Cl_2N_2O_2PZn$ (476.64): C, 47.88; H, 4.44; N, 5.88. Found: C, 47.96; H, 4.33; N, 6.08.

Synthesis of (DPEP)$_2$·PdCl$_2$ (5). $PdCl_2(C_6H_5CN)_2$ (0.19 g, 0.49 mmol) was allowed to react with **1** (0.34 g, 0.99 mmol) taken in dichloromethane (50 mL). A yellow solution was obtained. This was stirred at room temperature for 10 h and was filtered. Removal of solvent from the filtrate afforded a yellow powder (0.40 g, 92%): mp 262 °C. IR (KBr): 3056 (m), 2958 (m), 2921 (m), 1591 (m), 1553 (m), 1467 (sh, m), 1438 (s), 1313 (m), 1262 (sh, m), 1229 (vs), 1128 (s), 1040 (vs), 941 (s), 805 (s), 775 (s), 753 (s), 724 (s), 696 (s), 564 (s), 538 (s) cm^{-1}. IR (CH_2Cl_2): 3053 (m), 1678 (m), 1555 (m), 1438 (m), 1273 (m), 1227 (s), 1130 (s), 1037 (s), 940 (m), 748 (vs), 696 (m, sh), 560 (m), 533 (m) cm^{-1}. ^{1}H NMR ($CDCl_3$, ppm): δ 7.78−7.68 (m, 5H, *Phenyl*), 7.52−7.43 (m, 5H, *Phenyl*), 5.88 (d, 1H, *4H*−*Pyrazole*), 5.18(t, 2H, *OCH*$_2$), 4.99 (t, 2H, *NCH*$_2$), 2.67 (s, 3H, *CH*$_3$), 2.19 (s, 3H, *CH*$_3$). ^{31}P NMR ($CDCl_3$, ppm): δ 34.0 (s). Mass (FAB): 859(M^+). Anal. Calcd for $C_{38}H_{42}Cl_2N_4O_4P_2Pd$ (858.02): C, 53.19; H, 4.93; N, 6.53. Found: C, 53.35; H, 5.52; N, 6.79.

The hydrolytic stability of compounds **1**−**5** was evaluated in the following manner. The ^{31}P NMR of **1**, **4**, and **5** were recorded in $CDCl_3$ (vide supra). About 0.1 mL of D_2O was added to these solutions, and the ^{31}P NMR was recorded after 24 h. There was no change in the chemical shifts for any of the compounds. Also, no new peaks were detected. Further, compounds **1**−**5** (0.10 g) were dissolved in about 20 mL of CH_2Cl_2 and were treated with 0.5 mL of water. These solutions were stirred for 24 h at room temperature. Removal of solvent

(7) *Vogel's Textbook of Practical Organic Chemistry*, 5th ed.; Longman: London, 1989.
(8) Haanstra, W. G.; Driessen, W. L.; Reedijk, J.; Turpeinen, U.; Hamalainen, R. *J. Chem. Soc., Dalton Trans.* **1989**, 2309.

Table 1 [a]

	1[b]	**2**	**3**	**4**	**5**
empirical formula	$C_{38}H_{48}N_4O_7P_2$	$C_{19}H_{21}Cl_2N_2O_2P_1Co$	$C_{38}H_{42}Cl_2N_4O_4P_2Cu$	$C_{19}H_{21}Cl_2N_2O_2P_1Zn$	$C_{38}H42Cl_2N_4O_4P_2Pd$
fw	734.74	470.18	815.15	476.64	858.02
space group	*C*2/*c*	$P2_1/n$	$P\bar{1}$	$P2_1/n$	$P\bar{1}$
color of crystal	colorless	blue	dark green	colorless	yellow
crystal system	monoclinic	monoclinic	triclinic	monoclinic	triclinic
a (Å)	21.897(5)	9.751(6)	7.6780(18)	9.7530(20)	7.671(16)
b (Å)	10.009(2)	18.126(2)	11.455(3)	18.0247(20)	11.487(2)
c (Å)	19.147(9)	11.946(3)	11.782(3)	11.9998(20)	11.763(3)
α (deg)	90	90	97.525(16)	90	97.551(18)
β (deg)	111.40(3)	95.31(3)	90.09(2)	95.5162(80)	90.00(10)
γ (deg)	90	90	106.96(3)	90	106.87(8)
V (Å^3)	3907(2)	2102.4(14)	981.7(4)	2099.75(3)	982(2)
ρ_{calcd} (mg m^{-3})	1.249	1.485	1.379	1.508	1.450
Z	4	4	1	4	1
μ (mm^{-1})	0.163	1.163	0.818	1.517	0.734
λ (Å)	0.71073	0.71069	0.71073	0.71073	0.71073
T (K)	253(2)	293(2)	253(2)	193(2)	293(2)
GOF	1.065	0.923	1.293	1.296	0.935
total reflections	3457	2414	3682	9700	3717
independent reflns	2836	2273	3000	4533	3433
R_{int}	0.0254	0.0557	0.0168	0.0285	0.0160
R1 [$I > 2\sigma(I)$]	0.0436	0.0547	0.0373	0.0451	0.0284
wR2 [$I > 2\sigma(I)$]	0.1334	0.1817	0.1051	0.1528	0.0987

[a] $R = \sum||F_o| - |F_c||/\sum|F_o|$, $R_w = \{[\sum w(|F_o|^2 - |F_c|^2)^2]/[\sum w(|F_o|^2)^2]\}^{1/2}$. [b] **1** crystallizes with 1.5 molecules of H_2O.

from these reaction mixtures in vacuo afforded the starting compounds **1**−**5** in quantitative yields.

X-ray Crystallography. Crystals of **1**−**5** were obtained by the slow diffusion of *n*-hexane into solutions of these compounds in dichloromethane at room temperature in the absence of any precaution to prevent ingress of moisture. The process of crystallization took about one week. It was noticed that **1** crystallized with 1.5 molecules of water (vide infra). Deliberate addition of 2 mol of water during the above crystallization process of **1** also afforded the same crystals. The crystal data, data collection methodology, and refinement parameters for **1**, **2**, **3**, **4**, and **5** are given in Table 1. The X-ray diffraction data for **1**, **3**, and **4** were collected on a Bruker SMART diffractometer equipped with a CCD area detector. The structure was solved by direct methods using SHELXTL (5.10)[9] program and was refined by the least-squares method on F^2. For compounds **2** and **5**, X-ray diffraction data were collected on an Enraf Nonius FR590 CAD-4 diffractometer. The structure was solved by using the WINGX ver 1.63 crystallographic collective package (L. J. Farrugia, WINGX ver 1.63, An Integrated Systems of Windows programs for the solution, refinement and analysis of single-crystal X-ray diffraction data, Department of Chemistry, University of Glasgow). The structure was solved initially with SIR97 and was refined with the SHELX-97[10] package incorporated in WINGX. The structure was refined against F^2 with a full-matrix least-squares algorithm. All hydrogen atoms were included in idealized positions, and a riding model was used.

Results and Discussion

Synthesis. The ligand DPEP was prepared in a nearly quantitative yield by the reaction of diphenylphosphinic chloride with 1-(2-hydroxyethyl)-3,5-dimethylpyrazole in the presence of triethylamine as the hydrogen chloride scavenger (Scheme 1). DPEP shows a single phosphorus resonance at +32.9 ppm. In the proton NMR, the chemical shifts of the N−CH_2 and O−CH_2 protons are isochronous and resonate at +4.30 ppm. The methyl substituents on the pyrazole are nonequivalent and are seen as two singlets at 2.24 and 2.21 ppm, respectively.

The ligand DPEP has two potential coordination sites in the form of the phosphoryl oxygen and the pyrazolyl nitrogen. The possible modes of coordination are outlined in Scheme 2. Of these, the chelating mode does not appear to be favorable as it involves the formation of an eight-membered metallacycle. Exclusive coordination through the phosphoryl oxygens also is unlikely because of the presence of the strongly coordinating pyrazolyl nitrogens.

Scheme 1

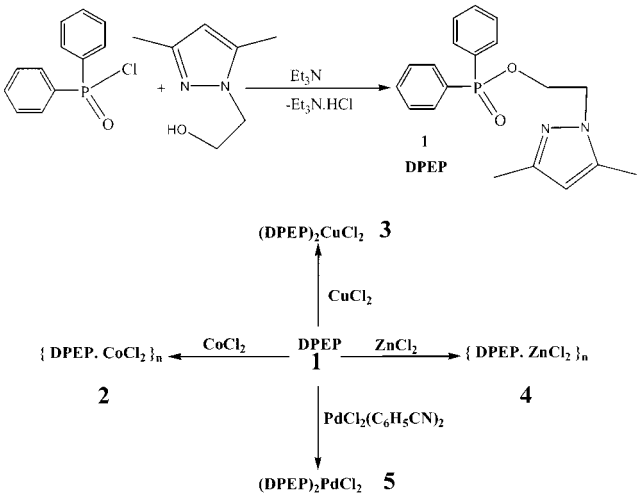

The reactions of DPEP with transition metal salts are insensitive to the stoichiometry of the reagents. Thus, in the reactions of DPEP with $ZnCl_2$ or $CoCl_2$ involving various stoichiometric combinations, only the 1:1 products are obtained. Similarly in the reactions with $CuCl_2$ or $PdCl_2(C_6H_5CN)_2$, only the 2:1 products are obtained (Scheme 1). The complexes **2**−**5** are nonionic in solution as determined by conductivity measurements, suggesting that the chlorides are bound to the metal ions in the complexes. Also, unlike the hydrolytic sensitivity of the metal complexes of phosphorus-based pyrazolyl ligands[2a,3,4] where the pyrazolyl group is directly attached to the phosphorus center, the complexes **2**−**5** are quite stable to moisture.

X-ray Crystal Structure of DPEP (1). The ligand crystallizes in the space group *C*2/*c* and contains four molecules in the unit cell. The molecular structure of **1** is shown in Figure

(9) Sheldrick, G. M. *SHELXTL, An Integrated System for Solving, Refining, and Displaying Crystal Structures from Diffraction Data*; University of Gottingen: Gottingen, Germany, 1991.
(10) Sheldrick, G. M. *SHELX-97, Program for Crystal Structure Refinement*; University of Gottingen: Gottingen, Germany, 1997.

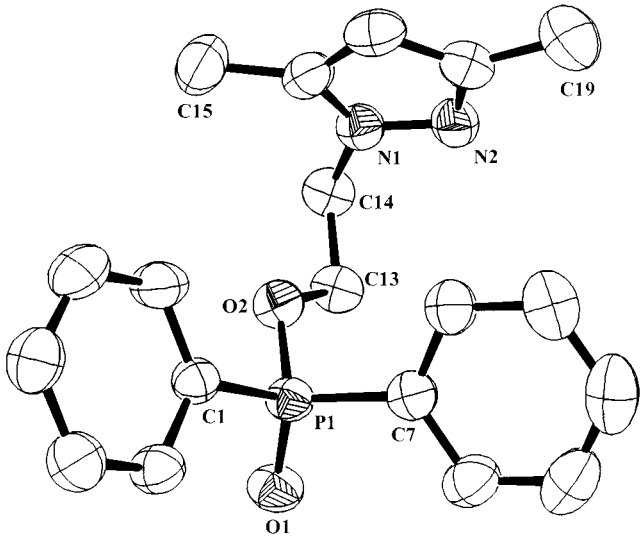

Figure 1. ORTEP plot of the ligand DPEP with thermal ellipsoids at 50% probability. Hydrogen atoms are omitted for clarity. Important bond lengths (Å) and bond angles (°) are P(1)−O(1) 1.4735(18), P(1)−O(2) 1.5874(19), O(1)−P(1)−O(2) 115.73(11), O(1)−P(1)−C(1) 113.47(11), O(2)−P(1)−C(1) 100.99(10), O(1)−P(1)−C(7) 111.15(12), O(2)−P(1)−C(7) 106.53(11), and C(1)−P(1)−C(7) 108.22(11).

Scheme 2

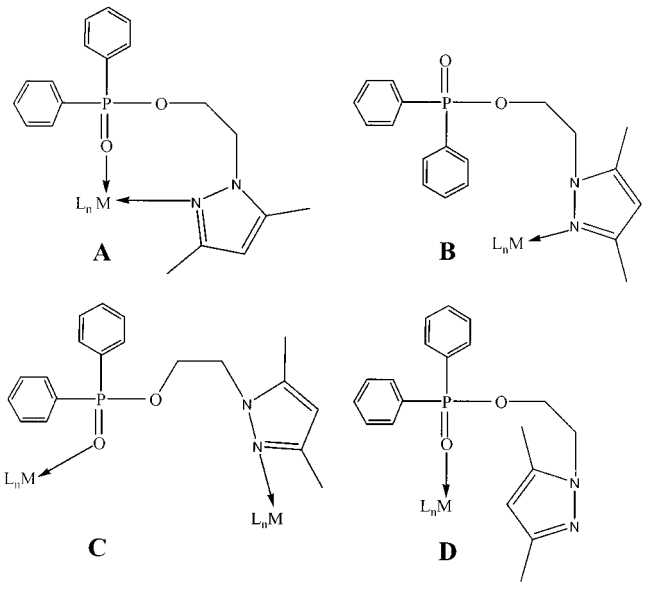

1. The two P−O bond lengths present in the molecule are not equal; P1−O1 is 1.4735(18) and P1−O2 is 1.5874(19) Å. The value of the P═O distance is sensitive to the substituents on phosphorus; the shortest distance observed is for $P(O)Br_3$ (1.44 Å).[11] In compounds that are related to DPEP, such as $(NH_2)_3P{=}O$[11] and $(C_6H_5)_2P(O)NMe_2$,[11] these distances have been measured to be 1.51 and 1.47 Å, respectively. The latter value is close to the one found in the present instance. The geometry around the phosphorus in DPEP is nearly tetrahedral; the shortest angle is the O2−P1−C1 angle of 100.99(10)°, and the largest angle is 115.73(11)° observed for O1−P1−O2 (Figure 1).

Two molecules of DPEP are involved in hydrogen bonding with three molecules of water of crystallization. The phosphoryl oxygen O1 is involved in a hydrogen bond with the H1 of a water molecule. A water molecule that lies on a center of inversion connects two DPEP·H_2O units affording a hydrogen-bonded chain as shown in Figure 2. The hydrogen bond distances O1−H1 [1.996(42) Å] and O3−H3 [1.963(9) Å] are perfectly normal. Also, the bond angles observed for these hydrogen bonds viz., O1−H1−O3 [171.03(2)°] and O3−H3−O4 [163.81(2)°], are in keeping with the hydrogen bonding trends known for O−H- - -O secondary interactions.[12]

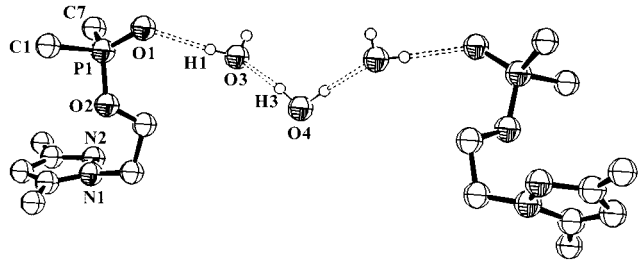

Figure 2. ORTEP plot of two molecules of DPEP hydrogen bonded through three water molecules. The phenyl rings and hydrogen atoms from the ligand are omitted for clarity. Important bond lengths (Å) and bond angles (°) are O(1)- - -H(1) 1.996(42), O(3)- - -H(3) 1.963(9), O(1)- - -O(3) 2.786(58), O(3)- - -O(4) 2.812(18), O(1)- - -O(4) 5.212(83), O(1)- - -O(1A) 9.618(181), O(1)−H(1)−O(3) 171.03(2), O(3)−H(3)−O(4) 163.81(2), O(1)−O(3)−O(4) 137.23(1), P(1)−O(1)−O(3) 128.47(1), O(3)−O(4)−O(3A) 119.32(1), and O(1)−O(4)−O(1A) 134.66(1).

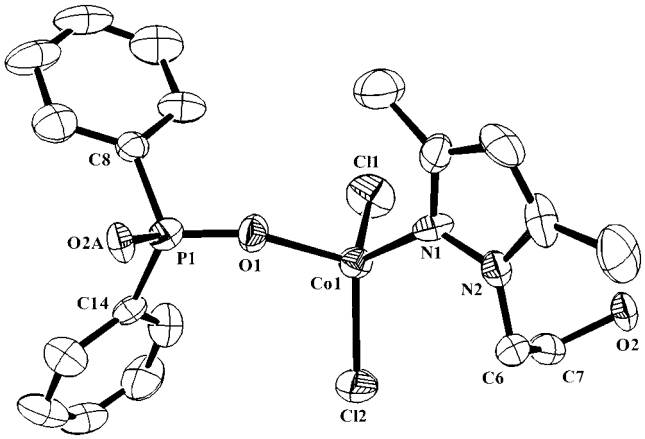

Figure 3. ORTEP plot of **2** showing the monomeric unit with thermal ellipsoids at 50% probability. Hydrogen atoms were omitted for clarity. Important bond lengths (Å) and bond angles (°) are Co(1)−Cl(1) 2.214(4), Co(1)−Cl(2) 2.229(4), Co(1)−O(1) 1.954(8), Co(1)−N(1) 2.031(11), P(1)−O(1) 1.490(9), P(1)−O(2) 1.578(9), O(1)−Co(1)−Cl(2) 109.7(3), N(1)−Co(1)−Cl(1) 110.7(3), Cl(2)−Co(1)−Cl(1) 111.7(18), O(1)−Co(1)−Cl(1) 105.6(3), O(1)−Co(1)−N(1) 103.2(4), N(1)−Co(1)−Cl(2) 115.2(3), and N(2)−N(1)−Co(1) 130.2(9).

X-ray Crystal Structures of (DPEP·$CoCl_2$)$_n$ (2) and (DPEP·$ZnCl_2$)$_n$ (4). Both cobalt(II) and zinc(II) chlorides form 1:1 complexes **2** and **4** with the tethered pyrazolyl phosphinate ligand DPEP. Compounds **2** and **4** are isostructural. The ORTEP diagram of **2** is shown in Figure 3. The coordination environment in **2** and **4** consists of two chlorine, one oxygen, and one nitrogen atoms arranged in a tetrahedral manner around the metal ion. The ligand DPEP acts in a bidentate bridging mode by linking two adjacent metal ions through its phosphoryl oxygen atom and the pyrazolyl nitrogen atom. This leads to the formation of a zigzag polymeric chain as shown in Figure 4A. The adjacent metal atoms within the polymeric chain are arranged alternately on either side of an imaginary axis running

(11) Corbridge, D. E. C. *The Structural Chemistry of Phosphorus*; Elsevier Scientific Publishing Co.: Amsterdam, 1974.

(12) Jeffrey, G. A.; Saenger, W. *Hydrogen Bonding in Biological Structures*; Springer-Verlag: Heidelberg, 1991.

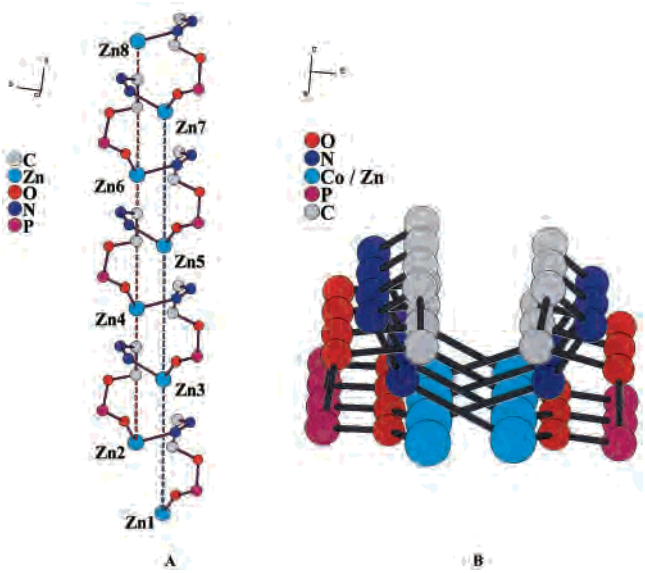

Figure 4. (A) DIAMOND view showing the zigzag arrangement of the polymer **4**. Only the atoms involved in chain propagation have been shown for clarity. The presence of two individual metal axis are marked in dotted lines. Important bond lengths (Å) and bond angles (°) are Zn(1)−Zn(2) 7.487, Zn(1)−Zn(3) 14.718, and Zn(1)−Zn(2)−Zn(3) 158.81. (B) DIAMOND view showing the rib-cage-like structural arrangement for the complexes **2** and **4**.

between the metal ions. This leads to an arrangement where the alternate metal ions perfectly eclipse each other as shown in Figure 4B and gives rise to an interesting situation where the *like atoms* on either half of the imaginary axis running between the polymer chain eclipse with each other to afford an overall rib-cage-like structure. Although polymeric complexes consisting of zinc and cobalt are previously known,[13] the type of polymeric architecture exhibited by **2** and **4** is unprecedented.

The adjacent metal separation in **2** (Co1−Co2) is 7.480 Å, while in **4** (Zn1−Zn2) it is 7.487 Å. The distance between the eclipsing metal atoms in **2** (Co1−Co3) is 14.705 Å, while in **4** (Zn1−Zn3) it is 14.718 Å. The metric parameters of **2** are summarized in Figure 3, while those of **4** are given in the Supporting Information. The P−O bond distance (P1−O1) corresponding to the phosphoryl oxygen increases to 1.490(9) Å in **2** and 1.496(2) Å in **4** and is consistent with the trends in the P═O stretching frequency observed in the infrared spectra of DPEP vis-à-vis the complexes **2** and **4** (vide infra).

X-ray Crystal Structures of $(DPEP)_2{\cdot}CuCl_2$ (3) and $(DPEP)_2{\cdot}PdCl_2$ (5). In contrast to the 1:1 complexes formed in the reactions between DPEP and $CoCl_2$ or $ZnCl_2$, the corresponding reactions with $CuCl_2$ or $PdCl_2(C_6H_5CN)_2$ proceed to afford exclusively 2:1 complexes **3** and **5** which are isostructural. The ORTEP diagram of **5** is shown in Figure 5.

The metal ions in **3** and **5** adopt a perfect square-planar geometry. The coordination environment around the metal ions consists of two chlorine and two pyrazolyl nitrogen atoms arranged in a trans configuration. Two DPEP ligands coordinate to one metal ion exclusively through the pyrazolyl nitrogens. The phosphoryl oxygen atoms are noncoordinating in contrast to the situation found for **2** and **4**. However, interestingly the

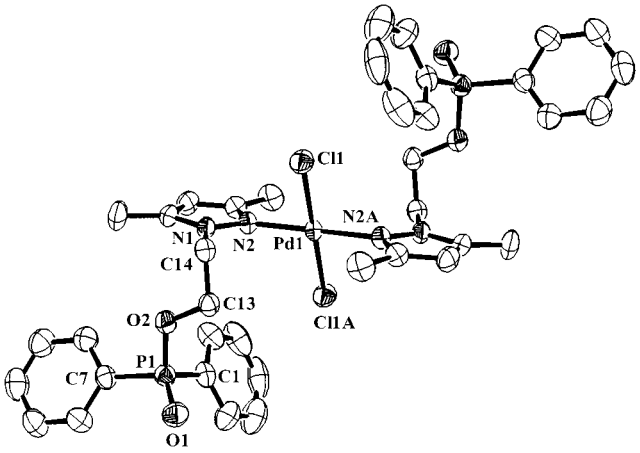

Figure 5. ORTEP plot of **5** with thermal ellipsoids at 50% probability. Hydrogen atoms were omitted for clarity. Important bond lengths (Å) and bond angles (°) are Pd(1)−Cl(1) 2.2904(9), Pd(1)−N(2) 2.011(4), Cl(1)−Pd(1)−Cl(1A) 180.00(4), N(2)−Pd(1)−N(2A) 180.00(8), Cl(1)−Pd(1)−N(2A) 90.58(10), Cl(1)−Pd(1)−N(2) 89.42(10), and N(1)−N(2)−Pd(1) 123.83(18).

two phosphoryl oxygen atoms (O1 and O1A in **5**) are in a perfect trans disposition with respect to each other. The M−O distances are 6.455 Å for **3** and 6.429 Å for **5**, respectively. The metric parameters found in the immediate coordination environment of **5** are summarized in Figure 5, while those of **3** are given in the Supporting Information. These are comparable to literature precedents.[14,15] The P1−O1 distance (1. 470(3) Å) for **5** and the analogous distance in **3** are completely unchanged in comparison to the value found for the free ligand DPEP consistent with the coordination situation found in these complexes.

A closer examination of the structures of **3** and **5** reveals extremely interesting intermolecular C−H- - -O secondary interactions between the phosphoryl oxygen and an aromatic C−H. This is shown for the copper complex **3** in Figure 6. Thus the phosphoryl oxygen O2 is hydrogen bonded to H12a (the meta hydrogen of the phenyl substituent on phosphorus of an adjacent molecule). The O2- - -H12a distance of 2.575 Å and the C12a−H12a−O2 bond angle of 147.28° for **3** (and the O1- - -H11 distance of 2.587 Å and the C11−H11−O1 angle of 147.95° for **5**) are quite reasonable for these kinds of interactions.[16] The effect of C−H- - -O interactions on the solid-state structures of organic and in some organometallic compounds has been recently reviewed.[17]

The consequence of C−H- - - -O interactions between two adjacent molecules is the formation of a rectangular box-type arrangement (Figure 6). In the absence of other effects, this would have been the only structural manifestation. However, as can be seen from Figure 7, a $\pi-\pi$, face-to-face, stacking interaction occurs between the phenyl groups associated with two immediate neighboring molecules leading to the formation of a polymeric chain. The $\pi-\pi$ centroid distance in the complex **3** is 3.883 Å, while in **5** it is 3.917 Å. The C−H- - -O

(13) (a) Borisov, G.; Varbanov, S. G.; Venanzi, L. M.; Albinati, A.; Demartin, F. *Inorg. Chem.* **1994**, *33*, 5430. (b) Ellis, W. W.; Schmitz, M.; Arif, A. A.; Stang, P. J. *Inorg. Chem.* **2000**, *39*, 2547. (c) Lu, J.; Paliwala, T.; Lim, S. C.; Lu, C.; Niu, T.; Jacobson, A. *Inorg. Chem.* **1997**, *36*, 923. (d) Lu, J.; Yu, C.; Niu, T.; Paliwala, T.; Crisci, G.; Somosa, F.; Jacobson, A. *Inorg. Chem.* **1998**, *37*, 4637.

(14) Hathaway, B. J. In *Comprehensive Coordination Chemistry*, 1st ed.; Wilkinson, G., Ed.; Pergamon Press: Great Britain, 1987; Vol. 5, p 533.

(15) Barnard, C. F. J.; Russell, M. J. H. In *Comprehensive Coordination Chemistry*, 1st ed.; Wilkinson, G., Ed.; Pergamon Press: Great Britain, 1987; Vol. 5, p 1099.

(16) Forristal, I.; Lowman, J.; Afarinkia, K.; Steed, J. W. *CrystEngComm* **2001**, *14*, 1.

(17) (a) Desiraju, G. R. *Acc. Chem. Res.* **1991**, *24*, 290. (b) Braga, D.; Grepioni, F.; Desiraju, G. R. *Chem. Rev.* **1998**, *98*, 1375.

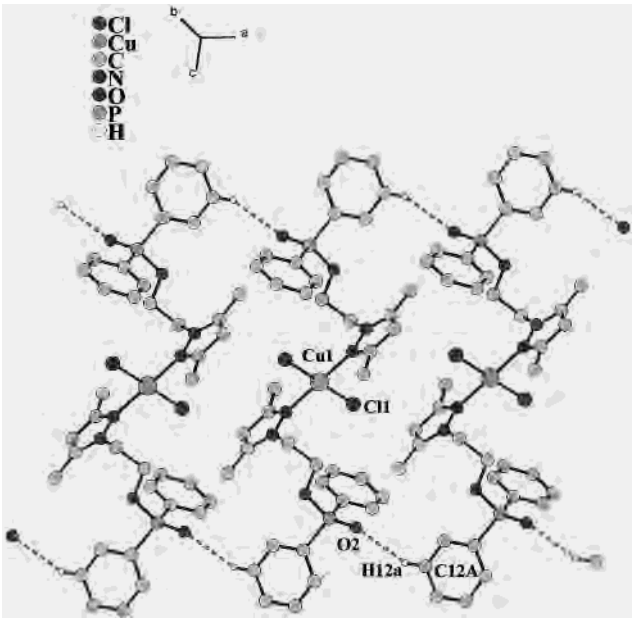

Figure 6. DIAMOND view of **3** showing the box-type polymeric network formed by the weak hydrogen bonds. Important bond lengths (Å) and bond angles (°) are O(2)- - - -H(12A) 2.575, O(2)- - - - -C(12A) 3.395, Cu- - - -Cu 7.678(2), and C(12A)−H(12A)−O(2) 147.28(2).

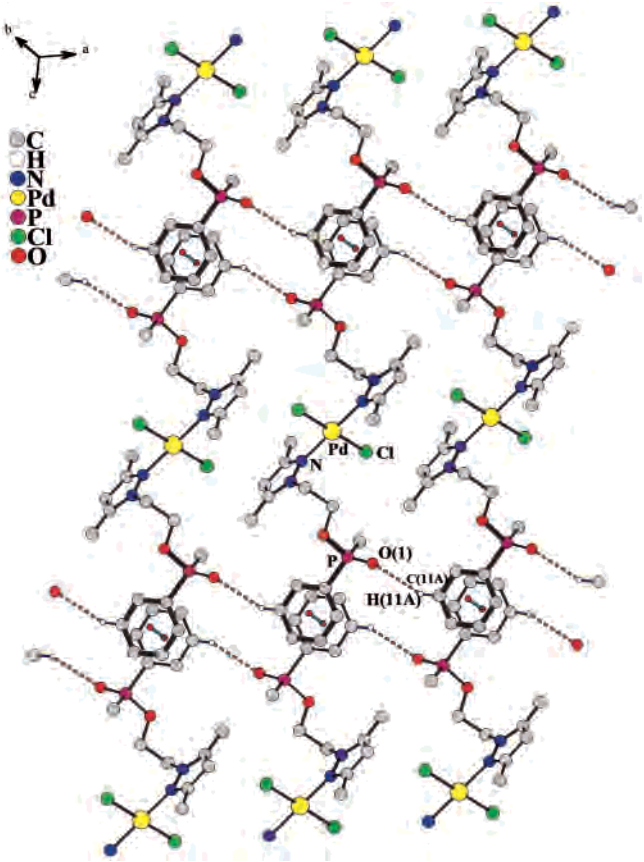

Figure 7. DIAMOND view of **5** showing the box-type polymeric network and the $\pi-\pi$ stacking arrangements. Only the hydrogen atoms and phenyl rings involved in weak bonding and in π stacking are shown for clarity. Important bond lengths (Å) and bond angles (°) are O(1)- - - -H(11A) 2.587, O(1)- - - -C(11A) 3.411, Pd- - -Pd 7.671(16), and C(11A)−H(11A)−O(1) 147.95(5); $\pi-\pi$(centroid−centroid) distance is 3.917.

interactions between the parallel polymeric chains result in a sheetlike two-dimensional polymeric network.

Table 2.

	P═O stretching frequency in cm^{-1}	
compound	in solid (KBr pellets)	in solution (DCM)
DPEP **1**	1223 (vs)	1226 (s)
2	1191 (vs)	1181 (s)
3	1226 (vs)	1223 (s)
4	1179 (vs)	1180 (s)
5	1229 (vs)	1227 (s)

Scheme 3

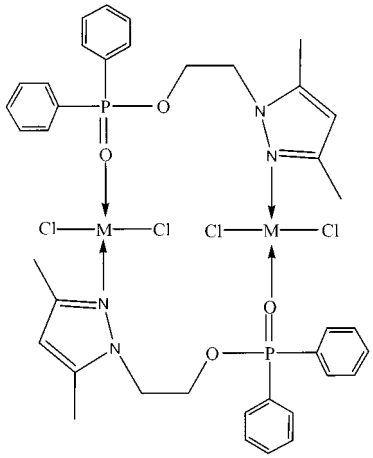

M= Co, Zn

Spectroscopic Aspects. The phosphorus chemical shifts of the diamagnetic complexes **4** and **5** are slightly deshielded in comparison to the ligand DPEP; the chemical shift of the zinc complex **4** is observed at +38.8 ppm, while that of the palladium derivative **5** is seen at +34.0 ppm. Also, in these metal complexes the O−CH_2 and the N−CH_2 resonances are resolved, and two distinct triplets are seen for each of these.

The P═O stretching frequency has been widely used as a diagnostic probe in determining the involvement of the phosphoryl oxygen in coordination to the metal ions. The P═O stretching frequency in the free ligand DPEP occurs at 1223 cm^{-1}. This may be compared to the values of 1200 cm^{-1} observed for the triamidophosphine oxide, $(NH_2)_3P{=}O$,[11] and 1165 cm^{-1} observed for dimethyl(aminomethyl)phosphine oxide, $(CH_3)_2P(O)CH_2NH_2$.[11] The P═O stretching frequency of **1** is shifted to 1191 and 1179 cm^{-1} for the cobalt (**2**) and zinc (**4**) complexes, respectively, corroborating the involvement of the phosphoryl oxygen atom in coordination to the metal ion in **2** and **4**. In the copper and palladium complexes **3** and **5**, where such an interaction is absent, the P═O stretching frequency remains almost unchanged in comparison to DPEP. The IR stretching frequency values for **1**−**5** are summarized in Table 2. As discussed vide supra these conclusions are borne out by the results of the single-crystal X-ray structure investigations. Solution IR for all of the complexes in dichloromethane shows that the P═O stretching frequency remains unchanged for these complexes in comparison with the solid-state values. This implies that the immediate coordination environment around the metal ions remains undisturbed in solution. The highest mass peaks observed in the electron-spray mass spectra of the cobalt and zinc complexes **2** and **4** occur at 905 and 917, respectively. These are due to singly charged ions of dimers from which a chlorine loss has occurred viz., $[(DPEP)_2{\cdot}COCl_2{\cdot}CoCl]^+$ and $[(DPEP)_2{\cdot}ZnCl_2{\cdot}ZnCl]^+$, respectively. The structures of the dimeric formulation for **2** and **4** are shown in Scheme 3 and are consistent with the solution IR data for these compounds (Table 2) which show that the P═O stretching

frequency in solution *also* occurs at a lower value in comparison to the ligand DPEP.

The EPR spectrum of the copper complex **3** as a glass in dichloromethane/toluene at 77 K shows that the $g_{||}$ value occurs at 2.370 with a corresponding $A_{||}$ value of 93.2 $\times$ 10^{-4} cm^{-1}. This value corresponds to a tetrahedral geometry around the copper. It is reasonable to suggest that the solid-state square-planar geometry observed for Cu(II) in **3** is probably due to the secondary interactions involving C−H- - -O hydrogen bonding and the $\pi-\pi$ stacking. Removal of these effects in solution or in a glassy state leads to a change to a tetrahedral geometry.

Acknowledgment. We are thankful to the Department of Science and Technology (New Delhi) for financial support.

Supporting Information Available: X-ray crystallographic files in CIF format for the structure determinations of DPEP (**1**), (DPEP·$CoCl_2$)$_n$ (**2**), (DPEP)$_2$·$CuCl_2$ (**3**), (DPEP·$ZnCl_2$)$_n$ (**4**), and (DPEP)$_2$·$PdCl_2$ (**5**); ORTEP diagrams and metric parameters of the complexes **3** and **4**. This material is available free of charge via the Internet at http://pubs.acs.org.

IC010454C